SRTTU

JCARME
ISSN: 2228-7922
Journal of Computational and Applied Research in Mechanical Engineering
Vol. 9, No. 1, pp. 1-18
jcarme.sru.ac.ir

# An advection-diffusion multi-layer porous model for stent drug delivery in coronary arteries

**S. M. Vahedi[a] , M. S. Valipour[a, *] and F. de Monte[b]**

[a] *Faculty of Mechanical Engineering, Semnan University, Semnan, Semnan Province, 35131-19111, Iran*
[b] *Department of Industrial and Information Engineering and Economics, University of L'Aquila, L'Aquila, Località Monteluco, 67040 Roio Poggio, Italy*

**Article info:**

Received: 01/07/2017
Accepted: 10/10/2018
Online: 14/10/2018

**Keywords:**
Multi-layer porous media,
Advection-diffusion equation,
Hypertension,
Pulsatile blood flow,
Drug-eluting stents,
Atherosclerosis.

**Abstract**

Arterial drug concentration distribution determines local toxicity. The safety issues dealing with Drug-Eluting Stents reveal the needs for investigation on the effective factors contributing to fluctuations in arterial drug uptake. The current study focuses on the importance of hypertension as an important and controversial risk factor among researchers on the efficacy of Heparin-Eluting Stents. For this purpose, the effect of blood pressure is systematically investigated in certain cardiac cycle modes. A comprehensive study is conducted on two classes, pulsatile (time-dependent), to have a more realistic simulation, and non-pulsatile (time-independent) blood flow, each one in four modes. The governing equations applied to drug release dynamics are obtained based on porous media theory. The equations are solved numerically using the Finite Volume Method. Results reveal that there is a significant difference when the plasma flow considered, and when it is neglected (regardless of time dependency). Moreover, the concentration level is more decreased in pulsatile blood flow rather than the non-pulsatile blood flow, although the penetration depth for pressure and concentration are nearly 20% and 5% of the wall thickness, respectively. In other words, the mass experienced by the arterial wall is lower in pulsatile blood flow in comparison to non-pulsatile blood flow. As a consequence, the risk of toxicity is declined as the blood pressure increases. Also, it can be seen that the polymer is diffusion-dominated so that no significant changes in the release characteristics are observed in the presence of the plasma filtration.

## Nomenclature

| | |
|---|---|
| $A$ | Geometric constants in Eq. (22) |
| $B$ | Geometric constants in Eq. (23) |
| $\tilde{C}_1$ | Maximum concentration at initial time (mg ml$^{-1}$) |
| $\tilde{c}$ | Drug concentration (mg ml$^{-1}$) |
| Courant | Courant number (-) |
| $D$ | Drug diffusivity (m$^2$ s$^{-1}$) |
| k | Partition coefficient (-) |
| $L_a$ | Arterial thickness (m) |
| $L_c$ | Coating thickness (m) |
| L | Thickness ratio (-) |
| m | Mass (-) |
| n | Number of volumes (-) |
| $\tilde{p}^0$ | Mean blood pressure (mmHg) |
| $\tilde{p}$ | Pressure (mmHg) |
| $P$ | Permeability of topcoat (m s$^{-1}$) |
| Pe | Peclet number (-) |
| $\tilde{t}$ | Times (s) |
| $\tilde{T}$ | Time period (s) |
| $U_{\text{ref}}$ | Reference filtration velocity calculated from |

[*] *Corresponding author*
*email address: msvalipour@semnan.ac.ir*

| | |
|---|---|
| | Eq. (7) in normal cardiac cycle ($m\ s^{-1}$) |
| $\tilde{u}$ | Filtration velocity ($m\ s^{-1}$) |
| VV | Non-dimentional parameter in Eq. (17) (-) |
| $\tilde{x}$ | Longitudinal coordinate (m) |

**Greek symbols**

| | |
|---|---|
| α | Hindrance coefficient (-) |
| Γ | Non-dimensional parameter in Eq. (16) (-) |
| ε | Porosity (-) |
| $\kappa$ | Darcy permeability ($m^2$) |
| $\lambda$ | Plasma isothermal compressibility($Pa^{-1}$) |
| $\mu$ | Plasma viscosity ($kg\ m^{-1}s^{-1}$) |
| σ | Porosity ratio (-) |
| Φ | Non-dimensional permeability (-) |
| γ | Diffusivity ratio (-) |

**Subscripts**

| | |
|---|---|
| i | *i*-th layer |
| $c$ | Coating |
| $a$ | Arterial wall |

**Superscript**

| | |
|---|---|
| ° | The average of systolic and diastolic blood pressure |

## 1. Introduction

Coronary Artery Disease (CAD), inextricably linked with Atherosclerosis, is the foremost cause of death, annually claiming the lives of 700,000 American people. Atherosclerosis, the cases of which grow each year, starts developing silently from childhood. Owing to the asymptomatic nature of the Atherosclerosis, it is not evident until myocardial infarction happens that the patient realizes he has CAD. As a matter of fact, the decrease in the coronary artery diameter and the subsequent oxygen shortage are the main reasons for a heart attack [1]. A myriad of invasive and non-invasive methods have been developed for the treatment of coronary artery stenosis, yet stent placement has been proven successful even for cases with more than 60% blockage [2]. Coagulant factors are activated by a wound which occurs during the stent inflation, consequently bringing about in-stent restenosis. Some researchers have suggested that the stent platform should be covered by an anti-restenotic drug which can entail anti-thrombogenic, immunosuppressive, anti-proliferative, anti-inflammatory and anticoagulant effects [1,3,4]. The reason why DES is employed more than Bare Metal Stents (BMS) is the former's ability to reduce in-stent restenosis by approximately 12%. The drug prevents Smooth Muscle Cells (SMC) migration by arresting the cell cycle [1,5,6]. Although several researchers give DES priority over BMS [6-9], others have questioned the long-term safety of DES [10-12]. Millions of patients worldwide have received DESs to reduce their risk for in-stent restenosis resulted from implanting BMSs. Toxicity can arise if an excessive amount of drug is delivered or if it is released too quickly. In other words, the local drug concentrations achieved are directly correlated with the biological effects and local toxicity, and establishing the optimum dose to be delivered to the tissue remains a challenge in today's DES design and manufacturing [9,10]. In order to lessen such confusion and answer the questions about the safety concerns surrounding DES, it is required to specify the local pharmacokinetics of drug and emphasize the importance of governing risk factors on the efficacy of DES [13].

The performance of Heparin-Eluting Stents (HES) has been rarely investigated in the open literature experimentally; however, some researchers investigated the pharmacokinetics of a drug by developing mathematical models [1,12,14,15]. In this regard, knowing the spatio-temporal tissue drug uptake in the arterial wall can provide very useful information about the pharmacokinetics of drugs which may, in turn, help designers making a high-efficiency DES [16,17]. Various assumptions, models, drugs, and geometries have been employed in the modeling of DES, which can be classified into three categories as follows:

- *No plasma filtration*: In this assumption, the plasma flow is ignored, hence resulting in the elimination of the convective term. Certain researchers have reported that convection is one order of magnitude lower than the diffusion [18-20].
- *Non-pulsatile plasma flow*: This approach, suggested by a steady interstitial plasma leakage in the arterial wall, is more realistic than the former. The pressure at the mural surface is considered the average of systolic and diastolic blood pressure and the pressure at the media-adventitia interface is considered as a fixed value. In spite of the arguments disregarding intramural plasma filtration, many researchers have taken convective term into account. Zunino studied the difference between hydrophilicity and hydrophobicity of

drugs in the presence of non-pulsatile plasma flow [21]. Pontrelli and de Monte [15] did systematic research on the convection and reaction terms, finding that employing the convective term renders the concentration profile flatter. The first study which simulated three-dimensional stent expansion was conducted by [22-24]. They considered the non-pulsatile intramural plasma filtration in a normal cardiac cycle, all unanimously reaffirming the importance of plasma flow.

- *Pulsatile plasma flow*: It is the most complete model for pressure oscillation consideration in each cardiac cycle studied by some of the researchers [25,26]. Chung and Vafai [25] used the sinusoidal function to simulate the oscillations of blood flow in their study on low density lipoprotein (LDL) transport. Kolachalama et al. [26] on their studies on DES have found that blood flow oscillations have more impact on the arterial drug distribution. However, two questions arise here. First, how much effect does blood oscillations have on the plasma filtration? Second, how much variation do hypertension and pulsatility impose to the drug pharmacokinetics?

The drug release either into the tissue or lumen has been considered by many researchers [4,10,19,20,26-31]. Although this is a challenging topic among researchers, some of them dedicated that luminal flow does not have a significant effect on the drug release into the tissue [29,30,32]. The effect of blood flow on drug transfer studied by Borghi et al. [30] in the case of heparin as a working drug. They showed that after 24h only about 0.002% of heparin is dissolved into the bloodstream. This assumption can be justified by the fact that stents are now routinely abluminally coated to reduce their washout which is mentioned by McGinty et al. [29]. According to their study, the dispersion of the drug into the lumen is not significant when recirculation zone in the proximal and distal of the strut goes to be vanished or minimized This happens when (1) the strut protrusion into the lumen is not remarkable, (2) the greater the vascular injury, the more the strut embedment into the wall [33], (3) things like remaining plaque, thrombus or tissue covers around the strut, (4) the surface which coated with the drug is just the abluminal one [29].

The pharmacological effects of the heparin,its tissue accumulation, duration, and distribution could potentially have an effect on the drug's efficacy. They can affect the delicate balance between the adequate amount of drug delivered over an extended period of time and minimal local toxicity needs to be struck [12, 29]. Thus, a deeper understanding of drug release is necessary for a rational design of the DES system. The main contributions of the present work with respect to previous research work can be summarized as follows:

- To the best of the authors' knowledge, heparin release dynamics from the DES has not yet been considered in pulsatile plasma flow.
- A single homogeneous porous medium simulated the arterial tissue and equations were developed.
- In the present paper, systematic study is conducted in two general classes, steady (non-pulsatile blood pressure) and unsteady blood flow (pulsatile blood pressure). In the first class, four modes with transmural pressure values of 70, 120, 160, and 180 mmHg are selected. Time-dependent blood pressure is created by adding a sinusoidal term with the amplitude of 25 mmHg and 1 s wavelength as the heartbeat to the mentioned values. Accordingly, four modes are presented for the second class.
- In the second class, pressure diffusion has to be solved, in addition to continuity and Darcy equations.
- A comprehensive comparison is then drawn between the two classes and the no-transmural plasma flow assumption. In-artery distribution of heparin (as the working drug) is computed and analyzed for the two classes.
- The effect of pressure oscillations is also investigated on the concentration in a single time period.
- The temporal variation of drug mass within both the polymeric gel and the arterial wall are studied under all conditions.
- The importance of the convective term is finally specified.

## 2. Mathematical formulation

### *2.1. Conceptual modeling*

A stent is a wire mesh cylinder with impermeable surfaces made of alloys. The heparin is loaded into a honeycombed polymer with 5 μm thickness. After the process of stenting is completed the stent is buried in the tissue. It is assumed that the arterial wall is clear against the plaques so that polymeric gel is in direct contact with the media layer via its topcoat.

The cross-section of the coronary artery is nearly circular with a diameter of 3mm, rendering negligible the circumferential variation of any properties. Three-dimensional geometry can, therefore, be reduced to two dimensions or one dimension when disregarding the axial variations. Moreover, since the ratio of polymer thickness to the arterial radiusis very small, 0.0033, it is only reasonable to employ a Cartesian coordinate system as has been widely used in substance transport studies [25,34-36]. Three models, describing the arterial wall, has been introduced in the literature as wall-free, lumen-wall and multi-layer structure [36]. The first one is the most simplified which the existence of the wall describes through boundary conditions. This model provides no information on the arterial drug distribution. The second model approximates the wall structure as a single homogeneous porous layer which is employed in the current study. In many analytical and numerical studies, this model has been used with great success [12,14,15,18,21,29,35,36,38]. The third one describing the actual anatomy of the arterial tissue is the most complicated model. However, non-homogeneity nature of the arterial wall is neglected in this study.

As depicted in Fig. 1, the lumen-wall model divides the computational domain into two parts with the Cartesian coordinate origin placed between the two domains (at the mural surface). The areas marked with letters (c) and (a) are the coating and the arterial wall, respectively. Letter (b) indicates the topcoat, a thin low-permeable free-drug membrane which its responsibility is to regulate drug release rate and thwarting the effect of less-controllable factors. The drug houses in the polymer with the concentration of $\tilde{C}_1$, at the time that there is no drug in the arterial wall. Drug elutes through the top coat, reaches the arterial wall and, with the passage of time, egresses from $\tilde{x} = \tilde{L}_a$ . During the release procedure drug mass into the polymer monotonically decreases. But, into the tissue, firstly drug increases, then reaches the maximum before it decreases. Its profile schematically is similar to Fig. 2. In pharmacy studies, the amount of drug in the tissue is divided into three domains of ineffective, effective, and toxic as Fig. 2 shows. Therefore, the researchers must consider the therapeutic window and control the dose of the drug between the ineffective and toxic limits.

Hydraulic properties of the polymer and arterial wall are listed in Table 1. So, to develop a mathematical model, the following assumptions have to be made:

- Strut has an impermeable surface against the plasma flow;
- Plasma flow just flows through the media layer;
- The blood pressure variations at the mural surface are modeled sinusoidal;
- The 1D Cartesian coordinate system is employed in the computational domain;
- The arterial wall is treated as a single homogeneous porous medium;
- The topcoat is modeled as a membrane so that the Kedem-Katchalsky equation is applied as a matching condition at the mural surface.

### *2.2. Governing equations*

According to the assumptions listed before, the mass balance of the drug in the coating and arterial wall (parts (c) and (a) in Fig. 1) are as follows:

$$\frac{\partial \tilde{c}_c}{\partial \tilde{t}} - D_c \frac{\partial^2 \tilde{c}_c}{\partial \tilde{x}^2} = 0 \quad \text{in} \quad [-\tilde{L}_c, 0] \tag{1}$$

$$\frac{\partial \tilde{c}_a}{\partial \tilde{t}} - D_a \frac{\partial^2 \tilde{c}_a}{\partial \tilde{x}^2} + \frac{\alpha_a u(\tilde{x}, \tilde{t})}{(k\varepsilon)_a} \frac{\partial \tilde{c}_a}{\partial \tilde{x}} = 0 \quad \text{in} \quad [0, \tilde{L}_a] \tag{2}$$

**Table 1.** Hydraulic and drug transport properties for both layers [14,36,37].

| **Parameters** | $D(\mathrm{m^2 s^{-1}})$ | $\tilde{L}(\mathrm{m})$ | $\varepsilon$ | k | $\alpha$ | $\kappa(\mathrm{m^2})$ | $\mu(\mathrm{kg\ m^{-1}s^{-1}})$ | $\lambda(\mathrm{pa^{-1}})$ | $P(\mathrm{m\ s^{-1}})$ |
|---|---|---|---|---|---|---|---|---|---|
| **Coating (*c*)** | $10^{-14}$ | $5\times10^{-6}$ | 0.1 | 1 | - | - | - | - | - |
| **Arterial wall (*a*)** | $7\times10^{-12}$ | $100\times10^{-6}$ | 0.61 | 1 | 1 | $2\times10^{-18}$ | $0.72\times10^{-3}$ | 4.5398 | - |
| **Topcoat** | - | - | - | - | - | - | - | - | $10^{-8}$ |

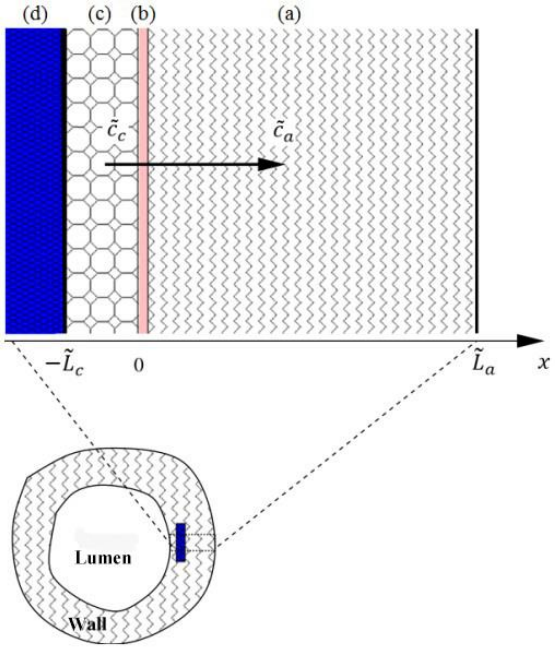


**Fig. 1.** A schematic representation of the computational domain; (a) arterial wall, (b) topcoat, (c) drug reservoir, and (d) stent strut [14].

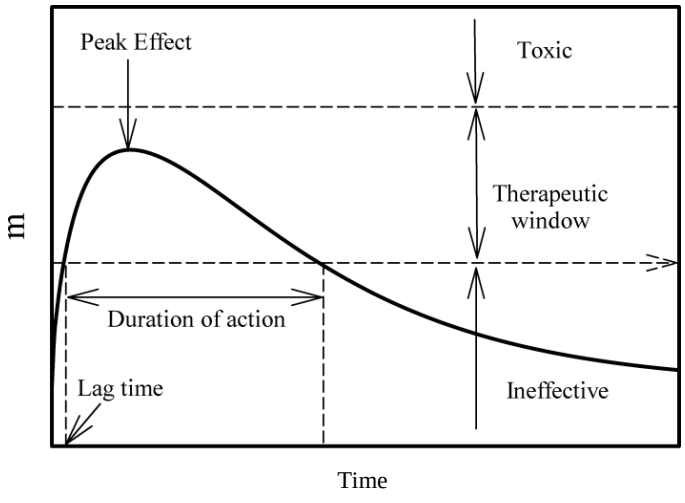


**Fig. 2.** The key characteristics of drug effect and relationship to the therapeutic window.

Pressure diffusion equation in the artery (part (a) in Fig. 1) is as follows:

$$\frac{\partial \tilde{p}}{\partial \tilde{t}} = \frac{\kappa}{\mu\lambda(k\varepsilon)_a}\frac{\partial^2 \tilde{p}}{\partial \tilde{x}^2} \quad \text{in} \quad [0, \tilde{L}_a] \tag{3}$$

Momentum equation or Darcy's law in the artery (part (a) in Fig. 1) is as follows:

$$\tilde{u}(\tilde{x}, \tilde{t}) = \frac{-\kappa}{\mu}\frac{\partial \tilde{p}}{\partial \tilde{x}} \quad \text{in} \quad [0, \tilde{L}_a] \tag{4}$$

In order to solve Eqs. (1-4), the following initial and boundary conditions are necessary:

*Initial conditions*

The concentrations of the drug along parts (c) and (a) (Fig. 1) of the domain are initially $\tilde{C}_1$ and 0, respectively as follows:

$$\tilde{c}_c(\tilde{x}, \tilde{t}) = \tilde{C}_1 \quad \text{at} \quad \tilde{t} = 0 \tag{5}$$

$$\tilde{c}_a(\tilde{x}, \tilde{t}) = 0 \quad \text{at} \quad \tilde{t} = 0 \tag{6}$$

Initial pressure distribution within part (a) (Fig. 1) is as follows:

$$\tilde{p}(\tilde{x}, \tilde{t}) = \left(\frac{\tilde{p}(L_a, \tilde{t}) - \tilde{p}(0, \tilde{t})}{\tilde{L}_a}\right)\tilde{x} + \tilde{p}(0, \tilde{t}) \quad \text{at} \quad \tilde{t} = 0 \tag{7}$$

*Boundary conditions*

The stent wall is impermeable, so the concentration flux must be zero on the strut surface.

$$-D_c\frac{\partial \tilde{c}_c}{\partial \tilde{x}} = 0 \quad \text{at} \quad \tilde{x} = -\tilde{L}_c \tag{8}$$

At the end of (a) region in Fig. 1, there is a perfect sink for the drug.

$$\tilde{c}_a = 0 \quad \text{at} \quad \tilde{x} = \tilde{L}_a \tag{9}$$

The pressure is time-independent at $\tilde{L}_a$, and equals to $p_{\mathrm{a}} = 30$ mmHg [36], that is,

$$\tilde{p}(\tilde{x}, \tilde{t}) = p_{\mathrm{a}} \quad \text{at} \quad \tilde{x} = \tilde{L}_a \tag{10}$$

*Interface condition*

The pressure at the mural surface needs more attention, and it can be identified in the general form as below:

$$\tilde{p}(\tilde{x}, \tilde{t}) = \tilde{p}^0 + \Delta p \sin\left(2\pi\tilde{t}/\tilde{T}\right) \quad \text{at} \quad \tilde{x} = 0 \tag{11}$$

where $\Delta p (= 25$ mmHg), $\tilde{T} (= 1$ s) , and $\tilde{p}^0$ are the amplitude of pressure oscillation, the duration of each heartbeat, and mean blood pressure, respectively [25]. Different values are assigned to $\tilde{p}^0$, each indicating a special cardiac cycle. The mean pressure in a normal cardiac cycle equals 100 mmHg, while the values, 150, 190, and 210 mmHg correspond to three hypertension modes [38].

Two interface conditions, the continuity of mass flux and Kedem-Katchalsky equation, for the drug concentration must be satisfied at the surface of topcoat.

$$-D_c\frac{\partial \tilde{c}_c}{\partial \tilde{x}} = -D_a\frac{\partial \tilde{c}_a}{\partial \tilde{x}} + \frac{\alpha_a \tilde{u}(\tilde{x}, \tilde{t})}{(\mathrm{k}\varepsilon)_a}\tilde{c_a} \quad \text{at} \quad \tilde{x} = 0 \tag{12}$$

$$-D_c\frac{\partial \tilde{c}_c}{\partial \tilde{x}} = P\left(\frac{\tilde{c}_c}{(\mathrm{k}\varepsilon)_c} - \frac{\tilde{c}_a}{(\mathrm{k}\varepsilon)_a}\right) \quad \text{at} \quad \tilde{x} = 0 \tag{13}$$

*2.3. Non-dimensional governing equations*

In order to generalize the results, it is better to non-dimensionalize all equations with initial and boundary conditions. Non-dimensional parameters can be defined as follows:

$$\mathrm{x} = \frac{\tilde{x}}{\tilde{L}_a}, \mathrm{L} = \frac{\tilde{L}_c}{\tilde{L}_a}, \mathrm{t} = \frac{D_a}{\left(\tilde{L}_a\right)^2}\tilde{t}, \mathrm{c}_c = \frac{\tilde{c}_c}{\tilde{C}_1}, \mathrm{c}_a = \frac{\tilde{c}_a}{\tilde{C}_1}, \gamma = \frac{D_c}{D_a}, \mathrm{u(x,t)} = \frac{\tilde{u}(\tilde{x}, \tilde{t})}{U_{\mathrm{ref}}}, \Gamma = \frac{\kappa}{D_a\mu\lambda(\mathrm{k}\varepsilon)_a}, \mathrm{p(x,t)} = \frac{\tilde{p}(\tilde{x}, \tilde{t})}{\tilde{p}\left(\tilde{L}_a, \tilde{t}\right)}$$

$$\mathrm{Pe}=\frac{\alpha_a U_{\mathrm{ref}}\tilde{L}_a}{(\mathrm{k}\varepsilon)_a D_a},\sigma=\frac{(\mathrm{k}\varepsilon)_c}{(\mathrm{k}\varepsilon)_a},\mathrm{VV}=\frac{\kappa\tilde{p}\left(\tilde{L}_a,\tilde{t}\right)}{\mu\tilde{L}_a^2 U_{\mathrm{ref}}},\phi=\frac{P\tilde{L}_a}{D_a(\mathrm{k}\varepsilon)_a}$$

where $U_{\mathrm{ref}}$ is a constant reference value for the filtration velocity calculated from the pressure initial condition in the normal cardiac cycle. By applying non-dimensional parameters to Eqs. (1-13), dimensionless equations can be derived as follows:

$$\frac{\partial \mathrm{c}_c}{\partial \mathrm{t}}-\gamma\frac{\partial^2 \mathrm{c}_c}{\partial \mathrm{x}^2}=0 \quad \text{in} \quad [-\mathrm{L},0] \tag{14}$$

$$\frac{\partial \mathrm{c}_a}{\partial \mathrm{t}}-\frac{\partial^2 \mathrm{c}_a}{\partial \mathrm{x}^2}+\mathrm{Pe}\,\mathrm{u}(\mathrm{x},\mathrm{t})\frac{\partial \mathrm{c}_a}{\partial \mathrm{x}}=0 \quad \text{in} \quad [0,1] \tag{15}$$

$$\frac{\partial \mathrm{p}}{\partial \mathrm{t}}=\Gamma\frac{\partial^2 \mathrm{p}}{\partial \mathrm{x}^2} \quad \text{in} \quad [0,1] \tag{16}$$

$$\mathrm{u}=-\mathrm{VV}\frac{\partial \mathrm{p}}{\partial \mathrm{x}} \quad \text{in} \quad [0,1] \tag{17}$$

Dimensionless boundary, initial and interface conditions can be rewritten as follows:

$$\mathrm{c}_c(\mathrm{x},\mathrm{t})=1 \quad \text{at} \quad \mathrm{t}=0 \tag{18a}$$

$$\mathrm{c}_a(\mathrm{x},\mathrm{t})=0 \quad \text{at} \quad \mathrm{t}=0 \tag{18b}$$

$$\mathrm{p}(\mathrm{x},0)=\left(\frac{\tilde{p}\left(\tilde{L}_a,\tilde{t}\right)-\tilde{p}(0,\tilde{t})}{\tilde{p}\left(\tilde{L}_a,\tilde{t}\right)}\right)\left(\frac{\tilde{x}}{\tilde{L}_a}\right)+\frac{\tilde{p}(0,\tilde{t})}{\tilde{p}(\tilde{L}_a,\tilde{t})} \quad \text{at} \quad \mathrm{t}=0 \tag{18c}$$

$$\frac{\partial \mathrm{c}_c}{\partial \mathrm{x}}=0 \quad \text{at} \quad \mathrm{x}=-\mathrm{L} \tag{18d}$$

$$\mathrm{c}_a=0 \quad \text{at} \quad \mathrm{x}=1 \tag{18e}$$

$$\mathrm{p}(\mathrm{x},\mathrm{t})=1 \quad \text{at} \quad \mathrm{x}=1 \tag{18f}$$

$$\mathrm{p}(0,\mathrm{t})=\frac{\tilde{p}^0}{\tilde{p}\left(\tilde{L}_a,\tilde{t}\right)}+\frac{25}{\tilde{p}\left(\tilde{L}_a,\tilde{t}\right)}\sin(2\pi\mathrm{t}/\mathrm{T}) \quad \text{at} \quad \mathrm{x}=0 \tag{18g}$$

$$-\gamma\frac{\partial \mathrm{c}_c}{\partial \mathrm{x}}=-\frac{\partial \mathrm{c}_a}{\partial \mathrm{x}}+\mathrm{Pe}\,\mathrm{u}(\mathrm{x},\mathrm{t})\mathrm{c}_a \quad \text{at} \quad \mathrm{x}=0 \tag{18h}$$

$$-\gamma\frac{\partial \mathrm{c}_c}{\partial \mathrm{x}}=\phi\left(\frac{\mathrm{c}_c}{\sigma}-\mathrm{c}_a\right) \quad \text{at} \quad \mathrm{x}=0 \tag{18i}$$

## 3. Solution methodology

Because of the complication of governing equations regarding the boundary and initial conditions, it is too difficult to solve them analytically, hence a numerical solution is in order.

### *3.1. Grid generation*

Fig. 3 shows the generated grids on the computational domain. In order to better capture the abrupt changes in concentration, the number of the cells should be increased at the mural surface. As shown in Fig. 3, $\Delta_{\mathrm{m}}$, which is the thickness of $m^{\mathrm{th}}$ cell, is calculated as follows;

$$\Delta_{\mathrm{m}}=0.5\frac{\Delta_1}{\mathrm{k}-1}(\mathrm{k}^{\mathrm{j}+1}-\mathrm{k}^{\mathrm{j}-1}) \quad \text{for} \quad \mathrm{i}=2,\dots,\mathrm{n}_1+\mathrm{n}_2+1 \tag{19}$$

where k and $\Delta_1$ respectively are the protraction ratio and the thickness of the first cell, which equals $2\delta_1$. Also, the thickness of the last cell is calculated as $2\left(\mathrm{L}-\mathrm{x}_{\mathrm{n}_1+\mathrm{n}_2+2}\right)$. The distance between the centers of $m^{\mathrm{th}}$ and $(m\text{-}1)^{\mathrm{th}}$ cells and the distance from the origin, respectively are given by the following equations:

$$\delta_{\mathrm{m}}=\frac{\Delta_{\mathrm{m}}+\Delta_{\mathrm{m}-1}}{2} \tag{20}$$

$$\mathrm{x}_{\mathrm{m}}=\Delta_1\frac{\mathrm{k}^{\mathrm{j}}-1}{\mathrm{k}-1} \tag{21}$$

The porosity difference of the layers and the presence of topcoat lead to a discontinuity in the concentration so that two nodes are defined at the mural surface labeled as $\mathrm{i}=\mathrm{n}_1+1$ and $\mathrm{i}=\mathrm{n}_1+2$. The former is assigned to the polymer, and the latter is assigned to the media tissue. Through the following relations, the concentration of the two nodes at each time step is calculated using the cells inside the computational domain.

$$\left.\frac{\mathrm{dc}}{\mathrm{dx}}\right|_{\mathrm{n}_1+1}=\mathrm{A}_1\mathrm{c}_{\mathrm{n}_1-3}+\mathrm{A}_2\mathrm{c}_{\mathrm{n}_1-2}+\mathrm{A}_3\mathrm{c}_{\mathrm{n}_1-1}+\mathrm{A}_4\mathrm{c}_{\mathrm{n}_1}+\mathrm{A}_5\mathrm{c}_{\mathrm{n}_1+1} \tag{22}$$

$$\left.\frac{\mathrm{dc}}{\mathrm{dx}}\right|_{\mathrm{n}_1+2}=\mathrm{B}_1\mathrm{c}_{\mathrm{n}_1+2}+\mathrm{B}_2\mathrm{c}_{\mathrm{n}_1+3}+\mathrm{B}_3\mathrm{c}_{\mathrm{n}_1+4}+\mathrm{B}_4\mathrm{c}_{\mathrm{n}_1+5}+\mathrm{B}_5\mathrm{c}_{\mathrm{n}_1+6} \tag{23}$$

where $\mathrm{A}_{\mathrm{i}}$ and $\mathrm{B}_{\mathrm{i}}$ are constants calculated by using the fifth-order Taylor expansion over the non-uniform grid as follows:

$$A_1 = \frac{x_{n_1-2}x_{n_1-1}x_{n_1}}{x_{n_1-3}(x_{n_1}-x_{n_1-3})(x_{n_1-1}-x_{n_1-3})(x_{n_1-2}-x_{n_1-3})} \quad (24)$$

$$A_2 = \frac{-x_{n_1-3}x_{n_1-1}x_{n_1}}{x_{n_1-2}(x_{n_1}-x_{n_1-2})(x_{n_1-1}-x_{n_1-2})(x_{n_1-2}-x_{n_1-3})} \quad (25)$$

$$A_3 = \frac{x_{n_1-3}x_{n_1-2}x_{n_1}}{x_{n_1-1}(x_{n_1-1}-x_{n_1-3})(x_{n_1-1}-x_{n_1-2})(x_{n_1}-x_{n_1-1})} \quad (26)$$

$$A_4 = \frac{-x_{n_1-3}x_{n_1-2}x_{n_1-1}}{x_{n_1}(x_{n_1}-x_{n_1-3})(x_{n_1}-x_{n_1-2})(x_{n_1}-x_{n_1-1})} \quad (27)$$

$$A_5 = -(A_1 + A_2 + A_3 + A_4) \quad (28)$$

$$B_1 = -(A_2 + A_3 + A_4 + A_5) \quad (29)$$

$$B_2 = \frac{x_{n_1+4}x_{n_1+5}x_{n_1+6}}{x_{n_1+3}(x_{n_1+6}-x_{n_1+3})(x_{n_1+5}-x_{n_1+3})(x_{n_1+4}-x_{n_1+3})} \quad (30)$$

$$B_3 = \frac{-x_{n_1+3}x_{n_1+5}x_{n_1+6}}{x_{n_1+4}(x_{n_1+6}-x_{n_1+4})(x_{n_1+5}-x_{n_1+4})(x_{n_1+4}-x_{n_1+3})} \quad (31)$$

$$B_4 = \frac{x_{n_1+3}x_{n_1+4}x_{n_1+6}}{x_{n_1+5}(x_{n_1+5}-x_{n_1+3})(x_{n_1+5}-x_{n_1+4})(x_{n_1+6}-x_{n_1+5})} \quad (32)$$

$$B_5 = \frac{-x_{n_1+3}x_{n_1+4}x_{n_1+5}}{x_{n_1+6}(x_{n_1+6}-x_{n_1+3})(x_{n_1+6}-x_{n_1+4})(x_{n_1+6}-x_{n_1+5})} \quad (33)$$

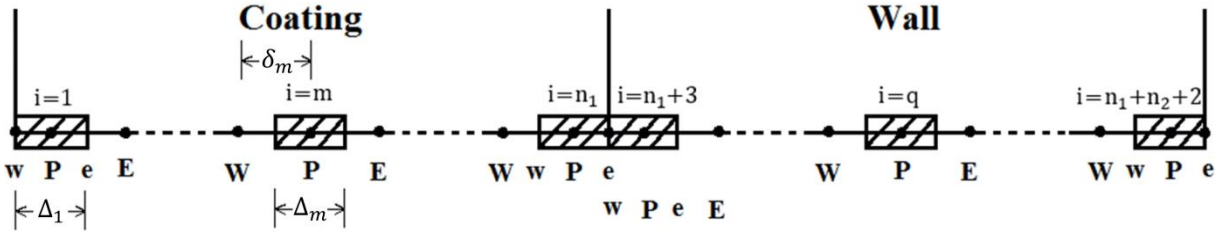


**Fig. 3.** A schematic representation of computational domain with control volumes.

**Table 2.** Grid study for six cases.

| Cases | Grid | | | | $m_a(t^*)$ | Percentage of deviation (%) |
|---|---|---|---|---|---|---|
| | Coating (*c*) | | Arterial wall (*a*) | | | |
| | Number of cells | Protraction ratio | Number of cells | Protraction ratio | | |
| 1 | 30 | 0.8030 | 100 | 1.0478 | 34.8098 | – |
| 2 | 50 | 0.8884 | 150 | 1.0280 | 34.8618 | 0.149 |
| 3 | 100 | 0.9510 | 200 | 1.0190 | 34.8718 | 0.028 |
| 4 | 150 | 0.9710 | 250 | 1.0136 | 34.8703 | 0.004 |
| 5 | 170 | 0.9750 | 270 | 1.0125 | 34.8698 | 0.001 |
| 6 | 200 | 0.9800 | 300 | 1.0105 | 34.8688 | 0.002 |

Substituting Eqs. (22 and 23) into Eqs. (18h) and (18i), the unknowns $c_{n_1+1}$ and $c_{n_1+2}$ are calculated. Since the arterial wall experiences a peak point (as shown in Fig. 2) at $t^*$ with the value of $m_a(t^*)$, this point is chosen in no-transmural plasma flow mode for checking the mesh independency. The results of grid study are listed in Table 2. By repeating the calculations with finer grids for parts (c) and (a), shown in Fig. 1, it can be revealed that the appropriate numbers of cells are 200 and 300, respectively, with the maximum error of 0.002%.

*3.2. Discretization method*

Finite Volume Method (FVM) in a fully explicit manner was applied to discretize the non-dimensional governing Eqs. (14-16) over the collocated grid of Fig. 3. Discretized continuity and pressure diffusion equations can be written as follows [39, 40]:

$$a_P {c_P}^{t+\Delta t} = a_W {c_W}^{t} + (a_P - a_W - a_E){c_P}^{t} + a_E {c_E}^{t} + b \quad (34)$$

$$a_P {p_P}^{t+\Delta t} = a_W {p_W}^{t} + (a_P - a_W - a_E){p_P}^{t} + a_E {p_E}^{t} + b \quad (35)$$

where $a_W$, $a_E$, and $a_P$ are coefficients listed in Table 3 for Eqs. (19 and 20). Once values at time step t are obtained, Eqs. (19 and 20) can be applied to achieve the value of concentration and pressure at the next time step, $t + \Delta t$. Therefore, these equations behave time-marching over time. The fraction of convection to diffusion does not exceed 1.4 in the most critical situation, namely under the highest blood pressure.

Accordingly, central differencing is used to discretize diffusion and convection terms [40]. The stability of the solution is controlled by three Courant numbers, correspond to Eqs. (14-16), which were appeared in discretization. Since a non-uniform grid is generated, each cell has a distinct Courant value that has to be less than 0.5 [39-41].

$$\mathrm{Courant}_1 = \frac{\gamma \Delta t}{\Delta \delta}; \quad \mathrm{Courant}_2 = \frac{\Delta t}{\Delta \delta}; \quad \mathrm{Courant}_3 = \frac{\Gamma \Delta t}{\Delta \delta} \quad (36)$$

*3.3. Verification of the numerical solution*

To solve the discretized governing equations, a code is developed using FORTRAN language. Results are verified via an analytical work done by Pontrelli and de Monte [14] where the transmural pressure is set to zero. In this case, the pressure diffusion equation and Darcy law are neglected. Fig. 4 shows that the results are in excellent agreement with the reported results of Pontrelli and de Monte [14].

**Table 3.** Coefficients of discretized continuity (Eq. (19)) and pressure diffusion (Eq. (20)) equations.

| | | Grid number | | | | | |
|---|---|---|---|---|---|---|---|
| | | Coating | | | Arterial wall | | |
| | | $i = 1$ | $i = m$ | $i = n_1$ | $i = n_1 + 3$ | $i = q$ | $i = n_1 + n_2 + 2$ |
| Continuity | $a_W$ | 0 | $\frac{\gamma_1}{\delta_m}$ | $\frac{\gamma_1}{\delta_{n_1}}$ | 0 | $\frac{\gamma_2}{\delta_q} + \mathrm{Peu}$ | $\frac{\gamma_2}{\delta_{n_1+n_2+2}}$ |
| | $a_P$ | $\frac{\Delta_1}{\Delta t}$ | $\frac{\Delta_m}{\Delta t}$ | $\frac{\Delta_{n_1}}{\Delta t}$ | $\frac{\Delta_{n_1+3}}{\Delta t} - \mathrm{Peu}$ | $\frac{\Delta_q}{\Delta t}$ | $\frac{\Delta_{n_1+n_2+2}}{\Delta t} + \mathrm{Peu}$ |
| | $a_E$ | $\frac{\gamma_1}{\delta_2}$ | $\frac{\gamma_1}{\delta_{m+1}}$ | 0 | $\frac{\gamma_2}{\delta_{n_1+4}} - \mathrm{Peu}$ | $\frac{\gamma_2}{\delta_{q+1}} - \mathrm{Peu}$ | 0 |
| | b | 0 | 0 | 0 | $2\mathrm{Peuc}_{n_1+3}$ | 0 | $-2\mathrm{Peuc}_{n_1+n_2+2}$ |
| Pressure diffusion | $a_W$ | - | - | - | 0 | $\frac{\Gamma}{\delta_q}$ | $\frac{\Gamma}{\delta_{n_1+n_2+2}}$ |
| | $a_P$ | - | - | - | $\frac{\Delta_{n_1+3}}{\Delta t}$ | $\frac{\Delta_q}{\Delta t}$ | $\frac{\Delta_{n_1+n_2+2}}{\Delta t}$ |
| | $a_E$ | - | - | - | $\frac{\Gamma}{\delta_{n_1+4}}$ | $\frac{\Gamma}{\delta_{q+1}}$ | 0 |
| | b | - | - | - | 0 | 0 | 0 |

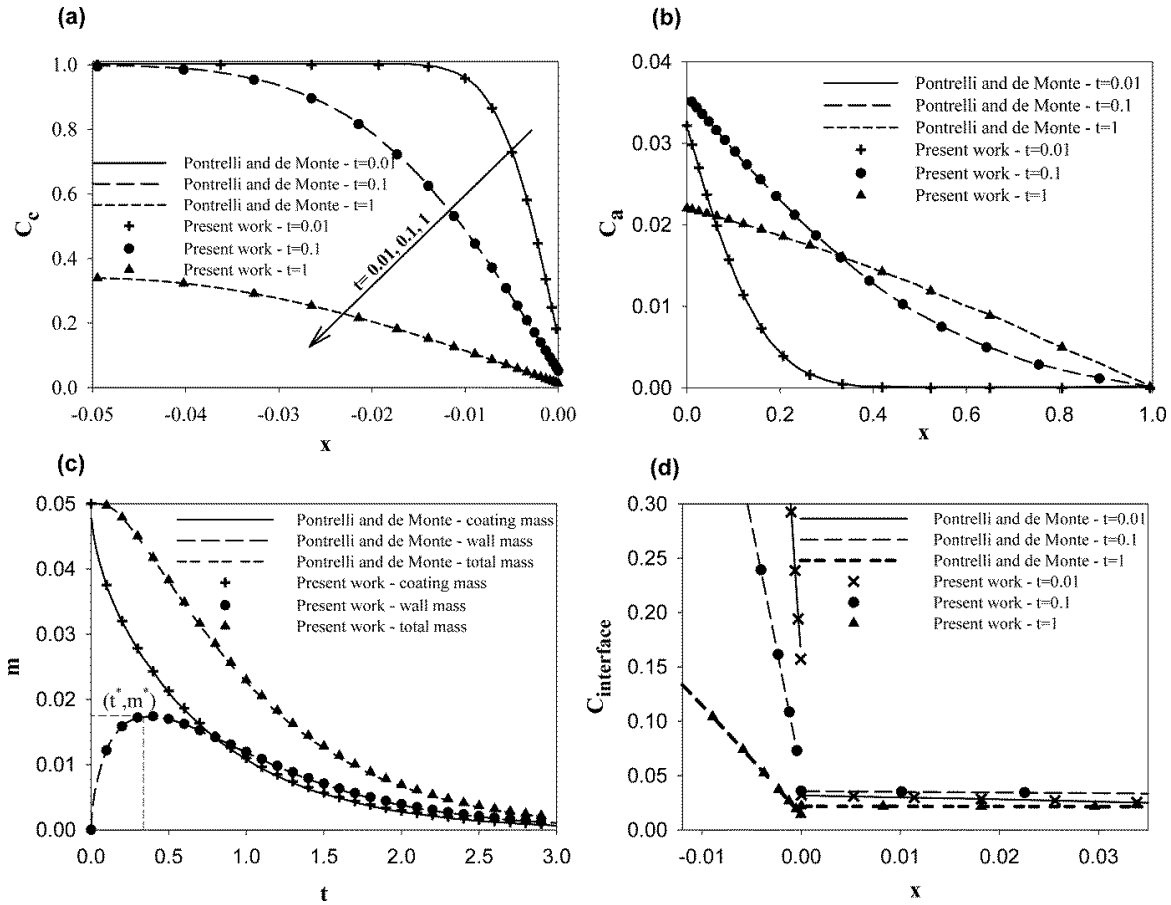


**Fig. 4.** Verifying the present study at Pe=0 with the analytical results of Pontrelli and de Monte [14]; (a) coating concentration, (b) wall concentration, (c) drug mass, and (d) concentration at the mural surface.

## 4. Results and discussion

Dimensionless parameters are calculated according to Table 1.

$\gamma = 0.0014$, $\sigma = 0.164$, $\phi = 0.234$, $L = 0.05$, $\Gamma = 1.4329 \times 10^{-4}$, $VV = 4285.7$ and $Pe = 6.07$.

### *4.1. Pulsatile and non-pulsatile blood flow*

According to Darcy's law, filtration velocity is due to the pressure gradient. For estimating the effect of pulsatile blood flow on drug release, the blood pressure is first assumed time-independent so that the pressure varies linearly along the media layer from $p^0$ at $x = 0$ to $p(1,t) = 1$ at $x = 1$. As expected, $p^0$ and u have different values at the four modes that are listed in table 4.

**Table 4.** Filtration velocity at different transmural pressures in non-pulsatile bood pressure.

| **Modes** | 1 | 2 | 3 | 4 |
|---|---|---|---|---|
| $\mathbf{p^0}$ | 3.33 | 5 | 6.33 | 7 |
| **u** | 1 | 1.714 | 2.286 | 2.572 |

Then, pressure oscillation at the mural surface is the key to solve pressure diffusion equation, the outcome of which is the pressure field. Pressure distribution for the first mode (namely, normal cardiac cycle) is calculated and plotted in Fig. 5(a). One time period has split up into eight equal distances, with $45^o$ phase variation. Interestingly, the penetration depth of the pressure variation barely reached $x = 0.2$. As a matter of fact, the pressure in the interval of 0.2 to 1 almost does not sense the effect of pulsation so that almost 20% of the arterial wall thickness is susceptible to pressure variation. Pressure oscillation penetration depth greatly and directly depends on Γ.

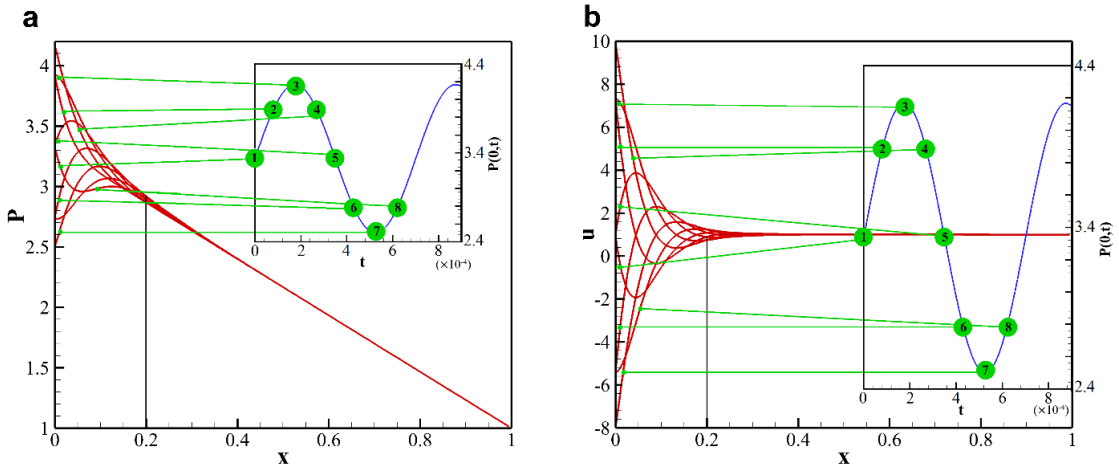


**Fig. 5.** (a) pressure and (b) filtration velocity distribution for eight points with 45 degree phase difference in a period.

It is obvious that each cell has a distinct value for filtration velocity which is calculated by the following equation:

$$u_i(x,t) = -VV\left(\frac{p_i - p_{i-1}}{\delta_i}\right) \quad (37)$$

Fig. 5(b) shows the filtration velocity for the eight points. Filtration velocity penetration depth does not exceed x=0.2 and tends to 1 beyond the zone. The amount of filtration velocity penetration depth depends on both Γ and VV. It is interesting to know that, by omitting the sinusoidal term $(0.833\sin(2\pi t/0.0007))$ there is no oscillation and the results tend to data tabulated in Table 4.

*4.2. Concentration and mass profiles*

Drug concentration and mass profiles in the layers (c) and (a), are the outcomes of solving the continuity equations. The impact of sinusoidal behavior on the pressure distribution, while heightened at the mural surface, is limited to the range of 0 to 0.2. The concentration is considerably affected by the pulsations in the vicinity of the mural surface. The first cardiac cycle mode in non-pulsatile form is selected, and the effect of time dependency on concentration variation is compared to non-pulsatile plasma flow. The results are depicted in Fig. 6, deeply in a period. Fig. 6 shows that just 5% of the tissue has an oscillatory concentration profilein the range of 0 to 0.05. Also, it can be seen that in short times, the concentration is higher in pulsatile blood flow than in non-pulsatile flow. However, regardless of the mentioned interval, time-dependent blood pressure decreases the concentration level. As a matter of fact, Γ, VV, and Pe determine the influence of pressure fluctuation on the continuity equation (Eq. (15)). The comparison of drug concentration in the arterial wall between the two classes and the case with no transmural pressure for all modes has been made and the results are depicted in Fig. 7. The existence of the convective term (without paying attention to pressure time-dependency) in the equations makes a big difference and helps flatten the concentration profiles. The mentioned difference, while negligible at first, is intensified over time. For instance, concentration profiles for time-independent and time-dependent classes are close to the concentration profile of no interstitial plasma flow at t=0.01. This difference becomes larger at t=0.1 and the highest at t=1. Therefore, the long-term response is highly affected by the plasma flow rather than acute response. Moreover, not only the concern of narrow therapeutic bound and vascular toxicity can be dismissed at higher blood pressure but also more sensitive drugs could be used for the patients suffering from hypertension.

In order to develop a successful DES, it is imperative that the coating should be designed so as to deliver, after stent implantation, a

therapeutic dose of the drug for the desired time duration at the site of the arterial blockage.
Thus, it is necessary to gain further insight into the impact of the blood pressure on the drug mass. The momentary integration of the concentration along the coating and the media layers result in coating and wall mass, respectively. Accordingly, the drug mass can be expressed as a function of time, $m(t)$. Non-dimensional mass in the coating, $m_c(t)$, and the arterial wall, $m_a(t)$, are plotted in Fig. 8. Focusing on the temporal variation of coating drug mass, it can be seen that transmural pressure in both classes does not significantly affect the available drug, a point that helps to clarify the importance of the topcoat. The dominant phenomenon in drug release dynamics from polymer is diffusion, so, it can be concluded that the adhesion of a drug-free polymer layer, called topcoat, creates a situation in which the coating is rendered independent of effective parameters like hypertension.

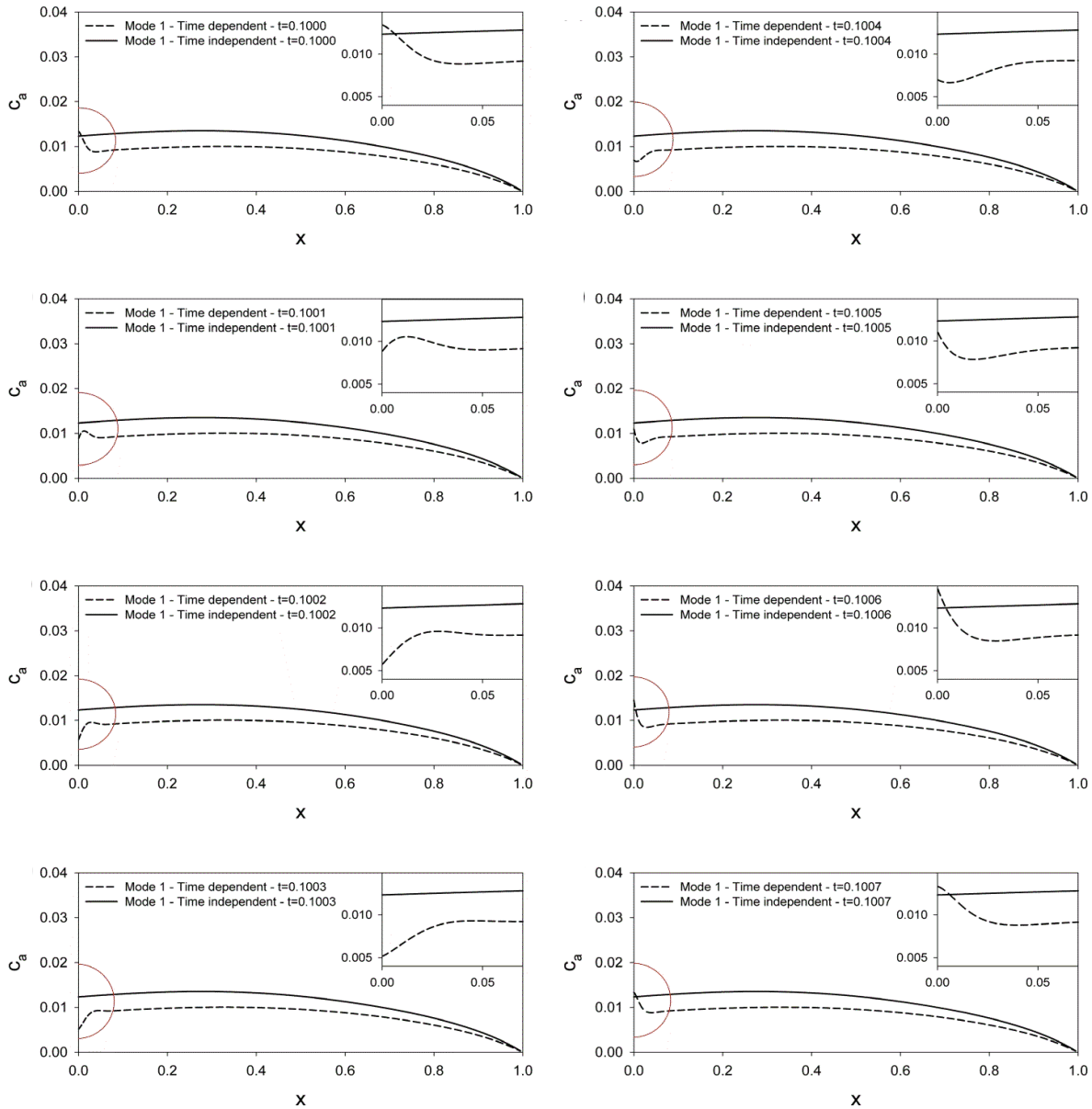


**Fig. 6.** Concentration variation profile in the arterial wall for pulsatile and non-pulsatile plasma flow in the normal cardiac cycle from t=0.1 in one period. The half circle located at the mural surface is the oscillating zone.

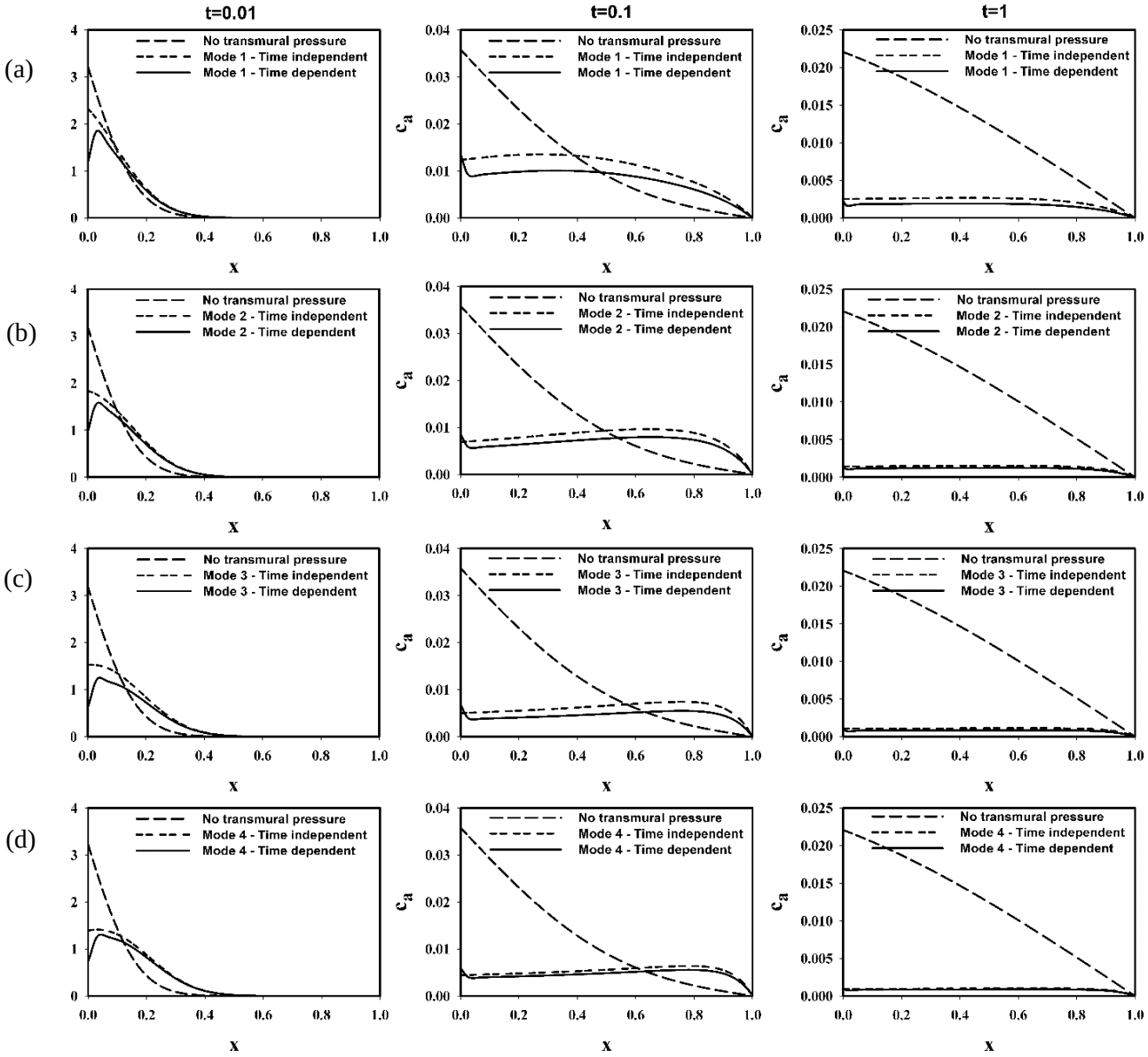


**Fig. 7.** Drug concentration distribution in the arterial wall for no-transmural, non-pulsatile and pulsatile plasma flows at t=0.01, t=0.1 and t=1 in the (a) first mode, (b) second mode, (c) third mode, and (d) fourth mode.

It can be seen from the right side graphs in Fig. 8 that the media tissue is free of the drug at first. However, the drug gradually diffuses this layer, and the amount of drug rises until it reaches its maximum level, $m(t^*)$, in a certain time, $t^*$. As the drug flux rises to $\tilde{L}_a$ and overcomes the drug flux at the mural surface, the drug depletion from the media layer starts until the layer becomes free of drug.

The right-hand side graphs in Fig. 8 shows a significant variation considering and neglecting the plasma flow regardless of its pulsation. As seen from the magnified illustrations in Fig. 8, the wall mass is rhythmically affected with the same frequency of concentration profile oscillations. It is also obvious that the dome shape of temporal variation of drug mass profile in the media layer becomes more compressed with lower peak point and the accumulated drug in the media layer decreases when the interstitial plasma flow took into account. According to the pharmacokinetic point of view, the DES designers must control the peak point not to exceed out of the therapeutic bound.

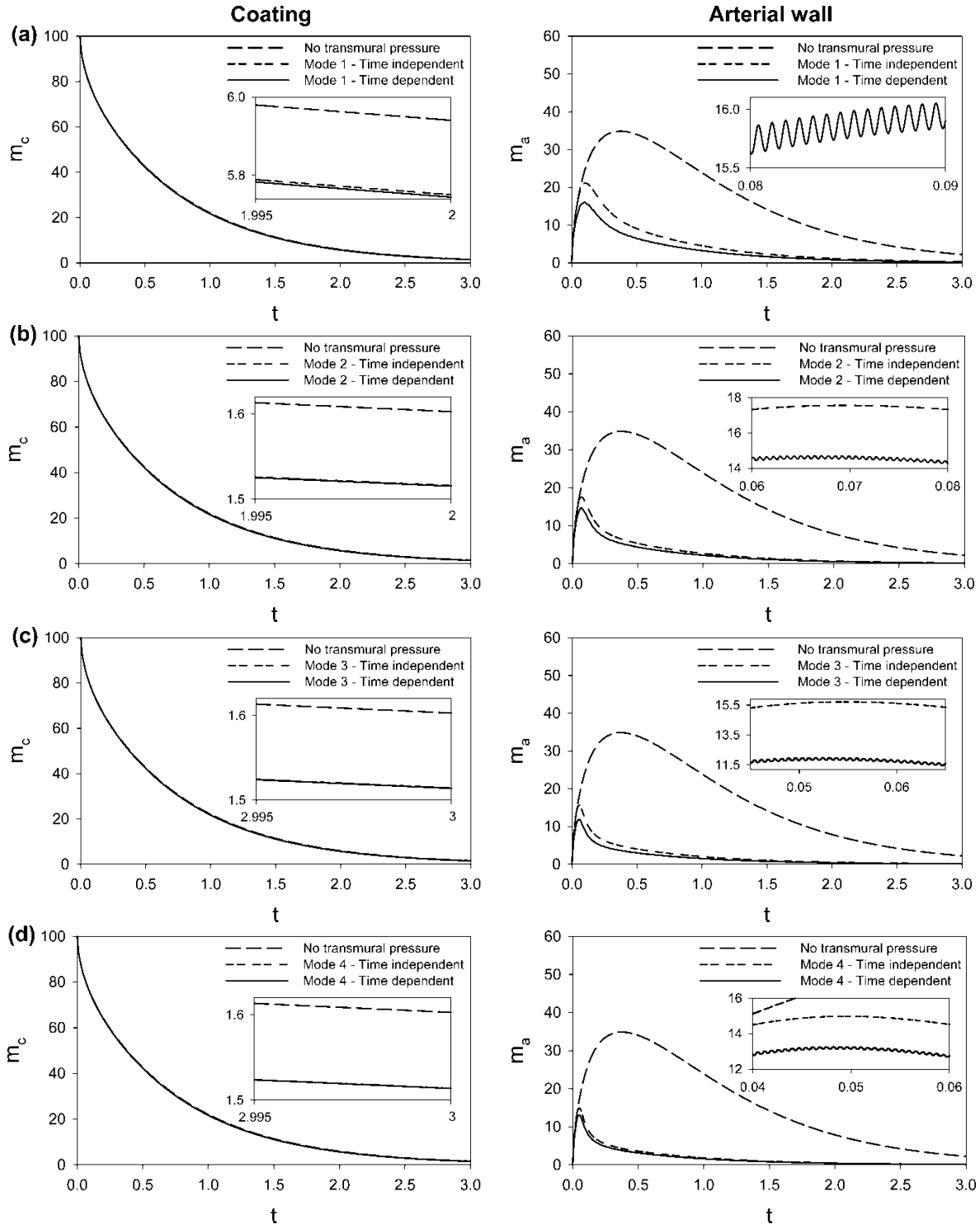


**Fig. 8.** Mass variations versus time for coating (left-hand side) and arterial wall (right-hand side) for no-transmural, non-pulsatile and pulsatile plasma flow in the (a) first mode, (b) second mode, (c) third mode, and (d) fourth mode.

**Table 5.** Peak effect characteristics, $m_a(t^*)$ and $t^*$, for the four modes in pulsatile and non-pulsatile plasma flow.

| | $m_a(t^*)$ | | | | $t^*$ | | | |
|---|---|---|---|---|---|---|---|---|
| Mode | 1 | 2 | 3 | 4 | 1 | 2 | 3 | 4 |
| Time independent | 21.153 | 17.558 | 15.716 | 14.982 | 0.106 | 0.069 | 0.054 | 0.049 |
| Deviation (%) | 39.33 | 49.64 | 54.92 | 57.03 | 71.45 | 81.42 | 85.46 | 86.80 |
| Time dependent | 16.091 | 14.711 | 11.991 | 13.271 | 0.099 | 0.049 | 0.045 | 0.048 |
| Deviation (%) | 53.85 | 57.81 | 65.61 | 61.94 | 73.34 | 86.80 | 87.88 | 87.07 |

The reference values for the calculations of deviation are 34.8688 and 0.3714 for $m_a(t^*)$ and $t^*$, respectively.

Heightened local arterial drug levels may be an especially potential problem given the narrow therapeutic window for heparin and its selective effects on smooth muscle cells. Assuming the peak point of the no transmural pressure profile as the threshold of toxicity, hypertension declines the risk of toxicity. The interventionists are offered using the HES with less concern of toxicity for patients suffering from hypertension. Allocating $t^*$ and $m_a(t^*)$ to the peak point, the impact of blood pressure on the maximum drug could be characterized and studied quantitatively. These values were tabulated in Table 5. It shows that transmural plasma flow has more effect on $t^*$ rather than $m(t^*)$. In time-independent blood

pressure class, both $t^*$ and $m_a(t^*)$ decrease monotonically with the increase in the transmural pressure. While in the second class, the same trend breaks down. It can be said that both $t^*$ and $m_a(t^*)$ primarily decrease, reaching their minimum in a pressure between 190 mmHg and 210 mmHg, then increase. It seems that, at higher blood pressures, the amplitude variation is the factor determining the change in monotonically trend. In other words, the sensitivity of $m_a(t^*)$ to the amplitude of oscillations becomes higher compared to the sensitivity to the transmural blood pressure. Generally speaking, the maximum amount of wall mass and its occurrence time are always lower in pulsatile blood flow.

## 5. Conclusions

Drug transport from the polymer-based heparin-eluting stents is systematically studied in normal and hypertensive cardiac cycles. The current study is formed in two classes, namely pulsatile and non-pulsatile blood flow, each consists of four cardiac cycle modes of 100, 150, 190, and 210 mmHg. Furthermore, in order to identify the existence of interstitial plasma flow, this model is compared with no intramural plasma filtration. The arterial wall and polymeric gel are simulated by two distinct homogeneous porous media. For this purpose, volume-averaged porous medium equations are applied to this modeling. The main outcomes of this study can be summarized as follows:

- Transmural plasma flow increases the drug transfer from the polymer-media interface to the depth of artery which causes a decrease in drug mass in the media layer. Plasma filtration (regardless of pulsatile or non-pulsatile blood pressure) is a necessary term must be considered for heparin-coated drug-eluting stents. The maximum amount of drug which is experienced by the arterial wall declines 39.33%, 49.64%, 54.92%, and 57.03% for the mentioned modes, respectively, in comparison to no plasma filtration.
- An increase in hypertension reduces the risk of arterial local toxicity.
- The lowest amount of maximum drug experienced by the arterial tissue is in pulsatile pressure in the range between 190mmHg and 210mmHg.
- As regards the available drugs, hypertension exerts undesirable effects because of the washout intensification.
- The interstitial plasma flow has much more effect on the long-term response rather than acute response.
- In comparison between pulsation and non-pulsation blood pressure, the results showed that, in the former, the drug is washed faster. In other words, the wall mass is at a lower level in pulsatile blood flow. Nonetheless, the mentioned difference is not significant, the

reason for which can be traced in the short transmural pressure penetration depth.

- Although there are enormous changes in pressure and velocity, especially near the polymer-media interface, the small values of groups $\kappa/\mu\lambda(k\varepsilon)_2$ and $\kappa/\mu$ reduce the effects of these fluctuations on concentration equation. Almost 5% of the arterial wall thickness has oscillatory concentration profiles in pulsatile plasma flow.
- The presence of topcoat makes the polymer as a diffusion dominated device.

## References


[1] B. M. O'Connell, E. M. Cunnane, W. J. Denny, G. T. Carroll and M. T. Walsh, "Improving smooth muscle cell exposure to drugs from drug-eluting stents at early time points: a variable compression approach", *Biomechanics and modeling in mechanobiology*, Vol. 13, No. 4, pp. 771-781, (2014).

[2] T. Shazly, V. B. Kolachalama, J. Ferdous, J. P. Oberhauser, S. Hossainy and E. R. Edelman, "Assessment of material by-product fate from bioresorbable vascular scaffolds", *Annals of biomedical engineering*, Vol. 40, No. 4, pp. 955-965, (2012).

[3] C. Yang, and H. M. Burt, "Drug-eluting stents: factors governing local pharmacokinetics", *Advanced drug delivery reviews*, Vol. 58, No. 3, pp. 402-411, (2006).

[4] R. Mongrain, I. Faik, R. L. Leask, J. RodĆ and O.F. Bertrand, "Effects of diffusion coefficients and struts apposition using numerical simulations for drug eluting coronary stents", *Journal of biomechanical engineering*, Vol. 129, No. 5, pp. 733-742, (2007).

[5] F. Alfonso, R. A. Byrne, F. Rivero and A. Kastrati, "Current treatment of in-stent restenosis", *Journal of the American College of Cardiology*, Vol. 63, No. 24, pp. 2659-2673, (2014).

[6] A. Kastrati, A. Dibra, C. Spaulding, G. J. Laarman, M. Menichelli, M. Valgimigli, E. Di Lorenzo, C. Kaiser, I. Tierala, J. Mehilli and M. Seyfarth, "Meta-analysis of randomized trials on drug-eluting stents vs. bare-metal stents in patients with acute myocardial infarction", *European heart journal*, Vol. 28, No. 22, pp. 2706-2713, (2007).

[7] C. Spaulding, P. Henry, E. Teiger, K. Beatt, E. Bramucci, D. Carrié, M. S. Slama, B. Merkely, A. Erglis, M. Margheri and O. Varenne, "Sirolimus-eluting versus uncoated stents in acute myocardial infarction", *New England Journal of Medicine*, Vol. 355, No. 11, pp. 1093-1104, (2006).

[8] G. J. Laarman, M. J. Suttorp, M. T. Dirksen, L. van Heerebeek, F. Kiemeneij, T. Slagboom, L. R. van der Wieken, J.G. Tijssen, B. J. Rensing and M. Patterson, "Paclitaxel-eluting versus uncoated stents in primary percutaneous coronary intervention", *New England Journal of Medicine*, Vol. 355, No. 11, pp. 1105-1113, (2006).

[9] F. Rikhtegar, E. R. Edelman, U. Olgac, D. Poulikakos and V. Kurtcuoglu, "Drug deposition in coronary arteries with overlapping drug-eluting stents", *Journal of Controlled Release*, Vol. 238, pp. 1-9, (2016).

[10] F. Bozsak, J. M. Chomaz and A. I. Barakat, "Modeling the transport of drugs eluted from stents: physical phenomena driving drug distribution in the arterial wall", *Biomechanics and modeling in mechanobiology*, Vol. 13, No. 2, pp. 327-347, (2014).

[11] D. M. Martin and F. J. Boyle, "Drug-eluting stents for coronary artery disease: a review", *Medical engineering & physics*, Vol. 33, No. 2, pp. 148-163, (2011).

[12] S. McGinty and G. Pontrelli, "A general model of coupled drug release and tissue absorption for drug delivery devices", *Journal of controlled release*, Vol. 217, pp. 327-336, (2015).

[13] B. M. O'Connell and M. T. Walsh, "Demonstrating the influence of compression on artery wall mass transport", *Annals of biomedical*

*Engineering*, Vol. 38, No. 4, pp. 1354-1366, (2010).

[14] G. Pontrelli and F. de Monte, "Mass diffusion through two-layer porous media: an application to the drug-eluting stent", *International Journal of Heat and Mass Transfer*, Vol. 50, No. 17, pp. 3658-3669, (2007).

[15] G. Pontrelli and F. de Monte, "Modeling of mass dynamics in arterial drug-eluting stents", *Journal of Porous Media*, Vol. 12, No. 1, pp. 19-28, (2009).

[16] C. J. Creel, M. A. Lovich and E. R. Edelman, "Arterial paclitaxel distribution and deposition", *Circulation research*, Vol. 86, No. 8, pp. 879-884, (2000).

[17] C. W. Hwang, D. Wu and E. R. Edelman, "Physiological transport forces govern drug distribution for stent-based delivery", *Circulation*, Vol. 104, No. 5, pp. 600-605, (2001).

[18] G. Pontrelli, A. Di Mascio and F. de Monte, "Local mass non-equilibrium dynamics in multi-layered porous media: application to the drug-eluting stent", *International Journal of Heat and Mass Transfer*, Vol. 66, pp. 844-854, (2013).

[19] P. Zunino, C. D'Angelo, L. Petrini, C. Vergara, C. Capelli and F. Migliavacca, "Numerical simulation of drug eluting coronary stents: mechanics, fluid dynamics and drug release", *Computer Methods in Applied Mechanics and Engineering*, Vol. 198, No. 45, pp. 3633-3644, (2009).

[20] B. Balakrishnan, J. F. Dooley, G. Kopia and E. R. Edelman, "Intravascular drug release kinetics dictate arterial drug deposition, retention, and distribution" *Journal of Controlled Release*, Vol. 123, No. 2, pp. 100-108, (2007).

[21] P. Zunino, "Multidimensional pharmacokinetic models applied to the design of drug-eluting stents", *Cardiovascular Engineering*, Vol. 4, No. 2, pp. 181-191, (2004).

[22] F. Migliavacca, F. Gervaso, M. Prosi, P. Zunino, S. Minisini, L. Formaggia and G. Dubini, "Expansion and drug elution model of a coronary stent", *Computer methods in biomechanics and biomedical engineering*, Vol. 10, No. 1, pp. 63-73, (2007).

[23] E. Cutrì, P. Zunino, S. Morlacchi, C. Chiastra and F. Migliavacca, "Drug delivery patterns for different stenting techniques in coronary bifurcations: a comparative computational study", *Biomechanics and modeling in mechanobiology*, Vol. 12, No. 4, pp.1-13, (2013).

[24] C. D'Angelo and P. Zunino, "Robust numerical approximation of coupled Stokes' and Darcy's flows applied to vascular hemodynamics and biochemical transport", *ESAIM: Mathematical Modelling and Numerical Analysis*, Vol. 45, No. 3, pp. 447-476, (2011).

[25] S. Chung and K. Vafai, "Effect of the fluid-structure interactions on low-density lipoprotein transport within a multi-layered arterial wall", *Journal of biomechanics*, Vol. 45, No. 2, pp. 371-381, (2012).

[26] V. B. Kolachalama, A. R. Tzafriri, D. Y. Arifin and E.R. Edelman, "Luminal flow patterns dictate arterial drug deposition in stent-based delivery", *Journal of Controlled Release*, Vol. 133, No. 1, pp. 24-30, (2009).

[27] B. Balakrishnan, A. R. Tzafriri, P. Seifert, A. Groothuis, C. Rogers and E. R. Edelman, "Strut position, blood flow, and drug deposition", *Circulation*, Vol. 111, No. 22, pp. 2958-2965, (2005).

[28] V. B. Kolachalama, E. G. Levine and E. R. Edelman, "Luminal flow amplifies stent-based drug deposition in arterial bifurcations", *PloS one*, Vol. 4, No. 12, p. e8105, (2009).

[29] S. McGinty, S. McKee, C. McCormick and M. Wheel, "Release mechanism and parameter estimation in drug-eluting stent systems: analytical solutions of drug release and tissue transport", *Mathematical Medicine and Biology*, p. dqt025, (2014).

[30] A. Borghi, E. Foa, R. Balossino, F. Migliavacca and G. Dubini, "Modelling drug elution from stents: effects of

reversible binding in the vascular wall and degradable polymeric matrix", *Computer Methods in Biomechanics and Biomedical Engineering*, Vol. 11, No. 4, pp. 367-377, (2008).

[31] G. Vairo, M. Cioffi, R. Cottone, G. Dubini and F. Migliavacca, "Drug release from coronary eluting stents: a multidomain approach", *Journal of Biomechanics*, Vol. 43, No. 8, pp. 1580-1589, (2010).

[32] X. Zhu, D. W. Pack and R. D. Braatz, "Modelling intravascular delivery from drug-eluting stents with biodurable coating: investigation of anisotropic vascular drug diffusivity and arterial drug distribution", *Computer methods in biomechanics and biomedical engineering*, Vol. 17, No. 3, pp. 187-198, (2014).

[33] J. K. Chesnutt and H. C. Han, "Simulation of the microscopic process during initiation of stent thrombosis", *Computers in biology and medicine*, Vol. 56, pp. 182-191, (2015).

[34] S. Wang and K. Vafai, "Analysis of low density lipoprotein (LDL) transport within a curved artery", *Annals of biomedical engineering*, Vol. 43, No. 7, pp. 1571-1584, (2015).

[35] S. Chung and K. Vafai, "Low-density lipoprotein transport within a multi-layered arterial wall-Effect of the atherosclerotic plaque/stenosis", *Journal of biomechanics*, Vol. 46, No. 3, pp. 574-585, (2013).

[36] S. Chung and K. Vafai, "Mechanobiology of low-density lipoprotein transport within an arterial wall-impact of hyperthermia and coupling effects", *Journal of biomechanics*, Vol. 47, No. 1, pp. 137-147, (2014).

[37] N. Zhang, P. Zhang, W. Kang, D. Bluestein and Y. Deng, "Parameterizing the Morse potential for coarse-grained modeling of blood plasma", *Journal of computational physics*, Vol. 257, pp. 726-736, (2014).

[38] N. Yang and K. Vafai, "Low-density lipoprotein (LDL) transport in an artery-A simplified analytical solution", *International Journal of Heat and Mass Transfer*, Vol. 51, No. 3, pp. 497-505, (2008).

[39] F. Khalighi, A. Ahmadi and A. Keramat, " Water hammer simulation by explicit central finite difference methods in staggered grids", *Journal of Computational and Applied Research in Mechanical Engineering*, Vol. 6. No. 2, pp. 69-77, (2016).

[40] Suhas V.Patankar, *Numerical Heat Transfer and Fluid Flow*, McGraw Hill, New York, USA, (1980).

[41] M. Alemi and R. Maia, "A comparative study between two numerical solutions of the Navier-Stokes equations", *Journal of Computational and Applied Research in Mechanical Engineering*, Vol. 6. No. 2, pp. 1-12, (2016).

**How to cite this paper:**

S. M. Vahedi, M. S. Valipour and F. de Monte, "An advection-diffusion multi-layer porous model for stent drug delivery in coronary arteries" *Journal of Computational and Applied Research in Mechanical Engineering*, Vol. 9, No. 1, pp. 1-18, (2019).

**DOI:** 10.22061/jcarme.2018.2741.1280

**URL:** http://jcarme.sru.ac.ir/?_action=showPDF&article=874